

An Automatic and Robust Algorithm for Segmentation of Three-dimensional Medical Images

Haibo Zhang and Hong Shen
Graduate School of Information Science
Japan Advanced Institute of Science and Technology
{haibo, shen}@jaist.ac.jp

Huichuan Duan
School of Information and Management
Shandong Normal University
hcduan@beelink.com

Abstract

Segmentation is a crucial precursor to most medical image analysis applications. This paper presents a new three-dimensional adaptive region growing algorithm for the automatic segmentation of three-dimensional images. The principle of our algorithm is to obtain a satisfactory segment result by self-tuning the homogeneity constraint step by step, which effectively resolves the dilemma of threshold auto-selection. Novel homogeneity and leakage detection criteria are designed to improve accuracy and robustness. Cavities auto-filling algorithm is also proposed to eliminate the interior cavities. Our algorithm was tested by segmenting lungs from 3D throat CT images and compared with manual segmentation and traditional 3D region growing. Results demonstrate that our algorithm greatly outperforms traditional 3D region growing method and its segment result is close to that of manual segmentation.

1. Introduction

Segmentation as the processing of labeling of objects in image data is a crucial step in many medical imaging analysis tasks, e.g., diagnosis, operation planning, as well as treatment delivery. With the development of X-ray computed tomography (CT) and magnetic resonance imaging (MRI), acquisition of 3D image is possible. Thus, it is critical to develop effective volumetric segmentation algorithms to support diagnosis or quantitative analysis.

Segmentation in medical imaging is generally considered a very difficult problem [1]. This difficulty mainly arises due to the sheer size of the datasets coupled with the complexity and variability of the anatomic organs. The situation is worsened by the shortcomings of imaging modalities, such as sampling artifacts, noise, low contrast etc. To support the clinical

workflow of today, it is essential to enhance the accuracy, automation and robustness of these methods.

3D region growing is a basic and effective method for volumetric image segmentation. However, 3D region growing still suffers some drawbacks despite its efficiency. First, its performance is highly dependant on a good choice of seeds. Secondly, the algorithm requires hand-tuning the homogeneity parameter, which is not robust and automatic. Thirdly, cavities will exist in the final segment result. Other drawbacks, such as limited reproducibility and demands for prior knowledge of the image structure, also hamper this algorithm's efficacy.

To address these problems, we propose an automatic, accurate and robust algorithm for extracting organs or interest regions from 3D images. The main contributions of this paper are described as follows:

- We design a novel and effective homogeneity criterion, which can greatly improve the segment accuracy.
- We present a leakage detection criterion to resolve the problem of over-segmentation.
- We propose a three-dimensional adaptive and iterative region growing algorithm (3DAIRG).
- We explore RLE (Run-length Coding) method to represent the final segment result. Cavity auto-filling algorithm based on this representation method is also presented.

The rest of the paper is organized as follows. Section 2 reviews some related work. In section 3, homogeneity criterion and leakage detection criterion are firstly derived, and then the three-dimensional adaptive and iterative region growing algorithm is presented in detail. Section 4 provides experimental results and analysis. Concluding remarks and directions for future work are given in the last section.

2. Related Work

Many researchers have been interested in region growing technique. Summers et al. [2] use 3D seeded region growing and a manually selected threshold to segment airways for rendering. The algorithm proposed by A.P. Kiraly et al. [3] uses a modified adaptive 3D region growing algorithm to extract lung regions from CT that automatically determines a threshold through repeated segmentations.

In addition, many contributions have also been done to overcome the drawbacks of region growing. A seeded region growing algorithm for two-dimensional image segmentation has been proposed in [4], however, the algorithm is highly dependent on the order of pixel processing. In [5], a model-based adaptive region growing algorithm was explored. However, this algorithm needs two runs of region growing.

An automated 3D region growing algorithm based on assessment function was presented in [6]. The principle of this algorithm is similar to ours. Unfortunately, the algorithm is only suitable to images with bimodal histogram. Our algorithm doesn't depend on the intensity distribution of image, and the threshold for homogeneity criterion is tuned automatically; furthermore, it can detect leakage during segmentation and less depends on the selection of seeds.

3. Method

3.1. Homogeneity Criteria Design

To perform region growing, criteria must be appropriately selected to effectively extract the regions. To make our algorithm more robust, we derive a novel homogeneity criterion considering both global and local similarity measurement.

Definition 1: $F_g(x, R)$, a function for calculating the similarity of the current voxel x with the target region R is defined as

$$F_g(x, R) = \exp\left(-\frac{(I_x - \bar{X}_R)^2}{2\sigma_R^2}\right)$$

where I_x is the intensity of voxel x , \bar{X}_R and σ_R denote the mean and standard deviation of region R respectively. Note that the similarity is determined by comparing the current voxel with the target region, so it is a global similarity measurement.

Definition 2: $F_l(x, N(x))$ is a function for calculating the similarity of the current voxel x with its neighbors, which is defined as:

$$F_l(x, N(x)) = \frac{\text{Card}(N_R(x))}{\text{Card}(N(x))} \exp\left(-\frac{(I_x - \bar{X}_{NR})^2}{2\sigma_{NR}^2}\right)$$

where $N(x)$ denotes the set of neighbors of the current voxel x , and 26-connected neighborhood is used in our algorithm. $N_R(x)$ represents the set of voxels that have been labeled as target voxels in $N(x)$. \bar{X}_{NR} and σ_{NR} correspond to the mean and standard deviation of $N_R(x)$ respectively. In this paper, we use $\text{Card}(A)$ to denote the cardinality (or voxel count) of set A . Note that only neighbors of the current voxel are considered in this function, so it is a local similarity measurement.

Definition 3: $F(x, N(x), R)$ is function for calculating the membership of the current voxel x belonging to the target region R . It is a linear combination of $F_g(x, R)$ and $F_l(x, N(x))$ using a weight parameter W .

$$F(x, N(x), R) = W \times F_g(x, R) + (1 - W) \times F_l(x, N(x))$$

Parameter W is a key factor that influences the performance of $F(x, N(x), R)$. Generally, the bigger $F_g(x, R)$ is, the voxel x has a higher similarity with the target region R . We use the following function to automatically calculate W when performing segmentation.

$$W = 1 - \exp\left(-\frac{F_g^2(x, R)}{2\sigma^2}\right), \quad 0 \leq F_g(I_x, R) \leq 1$$

In our paper, σ is set to 0.25, so that when $F_g(I_x, R) \rightarrow 1$, $W \rightarrow 1$

$$F(x, N(x), R) = \left[1 - \exp\left(-\frac{F_g^2(x, R)}{2\sigma^2}\right)\right] F_g(x, R) + \exp\left(-\frac{F_g^2(x, R)}{2\sigma^2}\right) F_l(x, N(x))$$

3.2. Leakage Auto-detection Criterion Design

Due to the complexity and variability of medical images, the case of not only having low-contrast, but also of weak edges at boundaries can be often encountered. Consequently, with no stoppage at weak edges, region growing algorithm is subject to leak. However, detection of leakage is fairly straightforward, and it is usually characterized by the sudden emergence of the following two properties:

(i) A large increase in the region size

Let T_F be the threshold for $F(x, N(x), R)$, and V_{T_F} represent the set of voxels of the volume acquired by 3D region growing with threshold T_F . According to the definition of homogeneity criterion $F(x, N(x), R)$, we can derive the following formula.

$\text{Card}(V_{T_F+\Delta}) \leq \text{Card}(V_{T_F}) \leq \text{Card}(V_{T_F-\Delta})$, where Δ is small positive value.

We use the following formula to detect leakage.

$$\frac{Card(V_{T_F-\Delta}) - Card(V_{T_F})}{\lambda Card(V) - Card(V_{T_F-\Delta}) + \eta}$$

Where λ is the estimated ratio of the target region size to the size of 3D image, and it can be estimated according to the knowledge of anatomy. η is a user-defined parameter which is used to control the detection sensibility.

(ii) A sharply change in the average intensity of border voxels.

If a region is surrounded by a border with higher (lower) intensity, the average intensity of border voxels will increase (decrease) dramatically when voxel growing is close to the border. Let $\bar{I}_B(T_F)$ be the average intensity of border voxels when the homogeneity threshold is equal to T_F . We define the following formula to avoid leakage.

$$\frac{|\bar{I}_B(T_F - \Delta) - \bar{I}_B(T_F)|}{\delta \bar{X}(R)}$$

where δ is also a hand-tuning parameter to control the detection sensibility.

In order to efficiently detect and void the leakage, both of the factors are taken into account. We define the auto-detection criterion as:

Definition 4: $F_E(T_F, R)$ is a function for calculating the possibility of leakage defined as

$$F_E(T_F, R) = \text{Max} \left\{ \frac{Card(V_{T_F-\Delta}) - Card(V_{T_F})}{\lambda Card(V) - Card(V_{T_F-\Delta}) + \eta}, \frac{|\bar{I}_B(T_F - \Delta) - \bar{I}_B(T_F)|}{\delta \bar{X}(R)} \right\}$$

If $F_E(T_F, R) > 1$, we deem that leakage occurs.

3.3. Three-dimensional Adaptive and Iterative Region growing Algorithm (3DAIRG)

3D adaptive and iterative region growing algorithm (3DAIRG) remedies the deficiencies that most region growing based algorithms are facing, and the principle of 3DAIRG is to obtain a satisfactory segment result by loosening the homogeneity constraint step by step.

To be specific, let $R(n)$ be the set of voxels belonging to the, up to now, formed regions in stage n and $B(n)$ represents the set of border voxels in $R(n)$.

Let $T_F(n)$ be the threshold for homogeneity criterion F and $\Delta(n)$ denote the decrement step of F in stage n . In this algorithm, we use a user-defined parameter θ to determine the termination of the algorithm. When $T_F(n) - T_F(n-1) < \theta$, the algorithm will be terminated. The segmentation accuracy can also be controlled by tuning θ .

In stage n , 3D region growing is performed. When a new voxel is added to $R(n)$, the average intensity and

standard deviation for $R(n)$, denoted as $\bar{X}(R(n))$ and $\sigma(R(n))$ respectively, will be updated at once according to the following equations.

$$\bar{X}(R'(n)) = \frac{\bar{X}(R(n)) \times Card(R(n)) + I_x}{Card(R(n)) + 1}$$

$$\sigma^2(R'(n)) = \frac{Card(R(n))}{Card(R(n)) + 1} \sigma^2(R(n)) + \frac{Card(R(n))}{[Card(R(n)) + 1]^2} [\bar{X}(R(n)) - I_x]^2$$

When no seeds exist or leakage has been detected, $\Delta(n)$ should change according to the following formula.

$$\Delta(n) = \begin{cases} \Delta(n-1) & \text{if } F_E(T_F, R) \leq 1 \\ \Delta(n-1)/2 & \text{if } F_E(T_F, R) > 1 \end{cases}$$

In the implementation of 3DAIRG, a FIFO (First In First Out) queue Q is used to store the seeds for segmentation. Another auxiliary structure is a cubical matrix, denoted as $Mask$. Now we can present the following three-dimensional adaptive and iterative region growing algorithm (3DAIRG) as follows.

Algorithm 1: 3D adaptive and iterative region growing algorithm (3DAIRG)

Step 1. Initialization

Mark seeds with 1 and non-seeds with 0 in $Mask$.

Set initial values for $T_F(0)$, $\Delta(0)$ and θ .

Step 2. Add seeds to $R(0)$, calculate $B(0)$, $\bar{X}(R(0))$ and $\sigma^2(R(0))$, $Q = B(0)$ and set iteration counter n with 1. $T_F(1) = T_F(0)$, $\Delta(1) = \Delta(0)$. $Leak = \text{False}$.

Step 3. While (not $Q.empty()$)

{ $P = Q.Get_First_Element()$

For (each neighbor x of P) do

If ($Mask(x) == 0$ && $F(x, N(x), R(n)) > T_F(n)$) then

{ Mark x with n in $Mask$.

Add x to Q .

Update $\bar{X}(R(n))$ and $\sigma^2(R(n))$. }

If $F_E(n, R) > 1$ then $Leak = \text{True}$; Break;

}

Step 4. If $Leak$ then

{ $B(n) = B(n-1)$; $\bar{X}(R(n)) = \bar{X}(R(n-1))$;

$\sigma^2(R(n)) = \sigma^2(R(n-1))$;

$T_F(n) = T_F(n-1) - \Delta(n)$; $\Delta(n) = \Delta(n)/2$;

Erase the labels in $Mask$ that have been marked with n , $Leak = \text{False}$; go to Step 6. }

else { $n++$; Update $B(n)$; }

Step 5. If $GrowSize(n) \neq 0$ then go to Step 3. // $GrowSize(n)$ is the count of voxels grown in stage n .

Step 6. If $T_F(n) - T_F(n-1) < \theta$ exit.

else { $T_F(n) = T_F(n-1) - \Delta(n)$, Go to Step 3. }

3.4. Segment Result Representation and Cavity Auto-filling Based on RLE

In this paper, we use a compact lossless representation method based on RLE. It permits complete reconstruction of the original segment result for later display. Also, it provides considerable information on the structure of the segment object.

A linear array is used to store the structure information of the segment result. Each element of the linear array is a tuple made up of 4-components, having the form of (x, y, z, l) , where (x, y, z) represents the voxel coordinate and l denotes the length of continuous labeled voxels from the voxel.

The RLE based representation also gives a means for straightforward efficient cavities filling. Suppose the tuples are searched along x axis (the same is to the other two axes). The detailed algorithm for cavities auto-filling is described as follows.

Algorithm 2. Cavities Auto-Filling Algorithm

Step 1. $P_1(x_1, y_1, z_1, l_1) = \text{Get_First_Elem}(\text{Array})$,
 $P_2(x_2, y_2, z_2, l_2) = \text{Get_Next_Elem}(P_1)$

Step 2. If $(z_1 = z_2) \& \& (y_1 = y_2)$ then

$$\{ \psi = |x_2 - x_1 - l_1|,$$

If $\psi < T$ remove $P_2(x_2, y_2, z_2, l_2)$ from Array and Set $l_1 = l_2 + (x_2 - x_1)$;

$$P_2(x_2, y_2, z_2, l_2) = \text{Get_Next_Elem}(P_1); \}$$

else $P_1(x_1, y_1, z_1, l_1) = P_2(x_2, y_2, z_2, l_2)$ and

$$P_2(x_2, y_2, z_2, l_2) = \text{Get_Next_Elem}(P_1)$$

Step 3. Repeat Step 2 until all tuples have been processed.

4. Results and Analysis

4.1. Application to Segment Lungs form 3D Thorax CT Images

The 3DAIRG algorithm was applied to segment lungs from 3D CT image of human thorax in order to analyze the lung parenchyma density, airway and lung mechanics. 3D CT images were obtained from an electron-beam CT scanner. Three typical image datasets are chosen to make comparison and their parameters are depicted in Table 1.

Table 1. 3D thorax CT image parameters

Image Name	Image Size (voxel)	Data Spacing (mm)		
		X	Y	Z
D1	512×512×62	0.593	0.593	5
D2	512×512×92	0.624	0.624	3
D3	512×512×92	0.684	0.684	3

Figure 1 shows the results of segmentation obtained by 3DAIRG. The seeds are automatically initialized using the method proposed in Section 3.5, and morphological erosion based post-processing is performed to eliminate improper seeds. As can be seen from Figure 1, the segment results are more satisfactory.

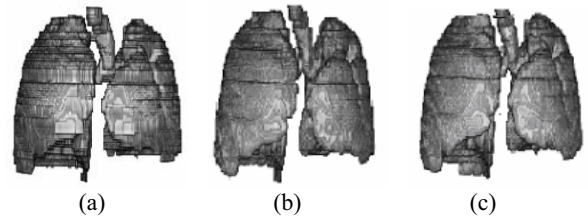


Figure 1. Lung segment results obtained by 3DAIRG. (a) D1, $\lambda = 0.07, \eta = 2000, \delta = 2, \Delta = 0.1, \theta = 0.01$. (b) D2, $\lambda = 0.067, \eta = 2000, \delta = 2, \Delta = 0.06, \theta = 0.001$. (c) D3, $\lambda = 0.067, \eta = 2000, \delta = 2, \Delta = 0.04, \theta = 0.001$.

We next evaluate the effectiveness of cavity auto-filling and segment result representation methods proposed in this paper. Figure 2 (b) gives the result obtained by the RLE based cavity filling method, and cavities have been completely eliminated. Figure 2(c) shows the result by morphological method used in [3]. Although the cavities have also been filled completely, the border has been extended and smoothed which will lose some information for the diagnosis of some disease on the lung surface.

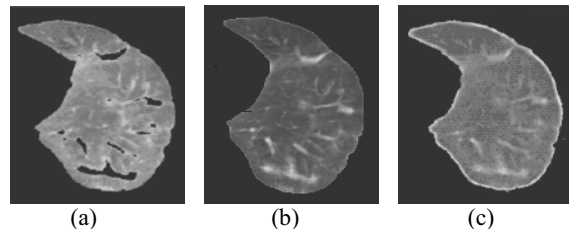


Figure 2. Cavities auto-filling results. (a) Original slice of right lung extracted from the segment results of D3. (b) Result obtained by RLE based cavity filling. (c) Result obtained by morphological method.

4.2. Comparison with Manual Analysis and 3D Region Growing

Segmentation accuracy was assessed by comparing 3DAIRG with manual segmentation and 3D region growing. Figure 3 shows the segment results for D3 using manual segmentation, 3D region growing, and 3DAIRG respectively. Figure 4 plots the comparison of mean distance between computer-defined (3DAIRG and 3D region growing) borders and the manually defined borders. As the results demonstrate, the result of 3DAIRG is much closer to that of manual method compared with traditional 3D region growing.

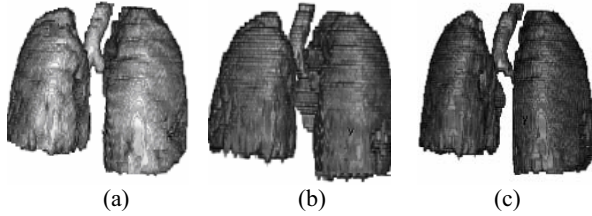


Figure 3. Segment result of D3 obtained by three different methods. (a) Manual segmentation. (b) 3D region growing with $T=243$. (c) 3DAIRG with $\theta = 0.0001$

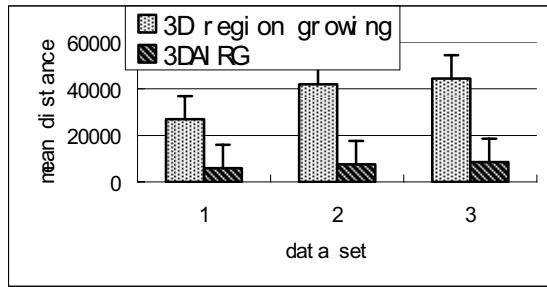


Figure 4. Comparison of mean distance for D1, D2 and D3.

4.3. Performance Analysis

The effectiveness of the homogeneity criterion is measured by comparing the average intensity of voxels grown in each stage. Figure 5 gives a description of this comparison. The average intensity of voxels grown in each step has an approximate increscent trend as the homogeneity constraint is loosened, which means that the criterion has a good measurement of the region homogeneity.

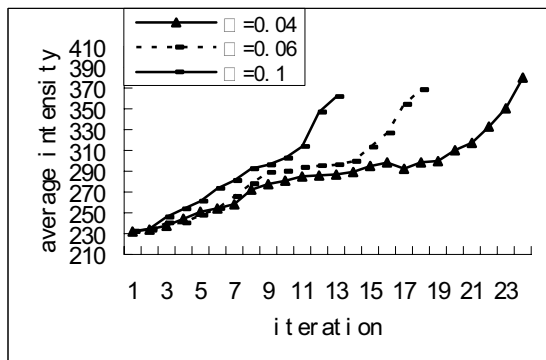


Figure 5. Average intensity of voxels grown in each stage by performing 3DAIRG on D3.

To verify the influence of parameter λ and δ to leakage detection, another 24 datasets have been tested, and we found that leakage can be effectively detected or avoided when δ ranges from 1.6 to 2.4 and λ falls in $[(1-9\%)\lambda_r, (1+11\%)\lambda_r]$, where λ_r is the real ratio of

the object size to the size of 3D image. Thus, 3DAIRG is more robust.

5. Conclusion and Future Work

In this paper we propose an automatic and robust algorithm—3DAIRG, which is based on 3D region growing, for segmentation of three-dimensional images. The principle of this algorithm is to obtain a satisfactory segment result by loosening the homogeneity constraint step by step with no need of hand-tuning the homogeneity parameter. The proposed algorithm was implemented for segmenting lungs from 3-D throat images and the results obtained are encouraging. However, the memory requirements are relatively high due to the huge size of 3D images and the execution time is also a little longer. Future research is directed toward the decrease of processing memory requirement and execution time.

References

- [1] Sarang Lakare, "3D Segmentation Techniques for Medical Volumes]", Research Proficiency, Department of Computer Science State University of New York at Stony Brook, 2000.
- [2] R. M. Summers, D. H. Feng, S. M. Holland, M. C. Sneller, and J. H. Shelhamer, "Virtual bronchoscopy: segmentation method for real-time display," *Radiology* 200, pp. 857-862, Sept. 1996.
- [3] A.P. Kiraly, W.E. Higgins, E.A. Hoffman, G.McLennan and J.M. Reinhardt, "3D Human Airway segmentation for virtual bronchoscopy". *SPIE Med. Imaging 2002: Physiology & Function in Multidimensional Images*. 4683, pp. 16-29, 2002.
- [4] R.Adams, L. Bischof, "Seeded Region Growing". *IEEE Trans. PAMI*, Vol.8, No.6 pp.641-647, June 1994.
- [5] Regina Pohle and Klaus D. Toennies, "A New Approach for Model-Based Adaptive Region Growing in Medical Image Analysis". *Lecture Notes in Computer Science*, Volume 2124 / 2001, 2001.
- [6] Chantal Revol-Muller, Francoise Peyrin, Yannick Carrillon and Christophe Odet, "Automated 3D region growing algorithm based on an assessment function", *Pattern Recognition Letters*, Volume 23, Issues 1-3, pp.137-150, January 2002.